

# Quasi-Optical Beamforming Approach Using Vertically Oriented Dielectric Wedges

Pratik Ghate\* and Jonathan Bredow

**Abstract**—Beamforming at mm-Wave and beyond is expected to be a critical need for many emerging applications such as Internet of Things (IoT), vehicular networking systems, and unmanned aerial navigation systems as well as 5G/6G backhaul communications. A new technique is proposed using quasi-optical beamforming that will address the shortcomings of existing beamforming approaches. These structures are passive (or nearly passive) having low cost, low power consumption, compact size and weight, have bandwidth advantages, and are expected to be able to operate at higher frequencies. The proposed structures give sufficient degrees of freedom to control the beamsteering angles by varying the dielectric constants and geometries of these structures and can form simultaneous multiple low overlapping beams. This approach increases the gain of the radiating source resulting in highly directive beams; our studies suggest that sufficient dielectric and shape parameters are available so that electrical tuning of beamformer parameters is possible. These structures are designed for a  $1 \times 3$  microstrip patch antenna to demonstrate the formation of three simultaneous low overlapping beams. The effects on bandwidth are negligible up to 4.4%, and scanning angle of  $180^\circ$  has been achieved by using vertically oriented dielectric wedges. 6 dB gain enhancement and the capability to scale to larger 2D arrays have also been demonstrated. Full wave simulation results in Ansys HFSS are provided to demonstrate the proposed techniques, and validation is done in CST MWS.

## 1. INTRODUCTION

Beamforming is a technique of forming single or multiple simultaneous beams that can be directed and shaped in specified directions. The concept of beamforming was introduced in 1905 by German physicist Karl Braun. Beamforming uses single or multiple antenna elements to control the directionality of transmission and reception of waves; in this case beamforming is achieved by appropriately adjusting the phase and magnitude of fields at the aperture from multiple antenna elements in an array via using a lens-like medium. By directing a signal in a specific direction, beamforming reduces interference and delivers higher amplitude signals to a receiver which in practice means faster information transfer [1–4]. Beamforming controls the directionality of the desired transmitted and received signals and mitigates interference.

Analog beamforming techniques such as Butler Matrix and Blass Matrix were introduced in the 1960's. Phase shifters, antennas, directional couplers, crossovers and transmission lines are used for the realization of these analog beamformers [10–12, 15–22]. The complexity of these networks for multiple beams and considerable insertion losses at higher frequencies make them undesirable at millimeter wavelengths. Microwave lens beamformers like Rotman lens, Ruze lens, and Luneburg lens were also invented in 1960's [6, 7, 14]. These structures are known as true time delay beamformers since their working principal is independent of frequency. Microwave lens type beamformers have the capability to form multiple minimally overlapping beams and have wide bandwidth; however, they are

---

*Received 25 July 2021, Accepted 26 September 2021, Scheduled 12 October 2021*

\* Corresponding author: Pratik Ghate (pratikbakul.ghate@mavs.uta.edu).

The authors are with the University of Texas, Arlington, USA.

not compact and cannot be used at higher microwave frequencies due to delay line complexities for large number of ports [8, 9]. Digital beamforming is the most widely adopted beamforming technique which is being used presently because of its low loss and scalability, plus facilitating adaptiveness to signal environments [13]. This technique has a large number of scanning steps and can form multiple simultaneous beams with each beam having a different amplitude and phase with minimum error. However, the simplest implementations require very fast A/D and D/A converters and strong digital processors which consume considerable power. In addition, to operate well into mm-wave frequencies additional frequency converting components are needed, increasing complexity and cost. Because of these limitations digital beamforming is not practical or cost effective for some applications, particularly at higher mm-wave frequencies. Hence, a more generalized low cost, passive (or nearly passive) quasi-optical approach that would work well at higher frequency ranges would be groundbreaking. For these structures' beams interact with lens type structures with a few wavelength dimensions, they can be referred to as "quasi-optical". Quasi optics involves beams of radiation propagating in free space; operations on these beams can be implemented directly using spatially distributed approaches such as amplifier and filtering arrays; these systems have been built for mmWave applications such as radar, plasma diagnostics, and astronomy for many years and have been proven to be a very important technology for multi-frequency antenna and beamforming systems.

As the operating frequency increases and communication and sensing applications will move well into mmWave frequencies, many conventional beamforming techniques will be unable to meet needed specifications [5]. To address these limitations, many alternatives such as partially reflective surfaces, shaped dielectrics, and metamaterials were explored and are considered potential candidates for inhomogeneous lens type structures to perform the beamforming operation [23, 24]. Simulations to date have demonstrated beam shaping and beamsteering using metamaterials in partially reflective surfaces [25–28]. The use of partially reflective structures with appropriate shapes has shown the increase of 67% in antenna directivity. Incorporating nonplanar metamaterial structures has demonstrated beamsteering capability of  $\pm 30$  degrees [29–34]. The proposed quasi-optical approach is expected to enhance performance of components in emerging systems such as broad deployment of 5G backhaul communications, Internet of Things (IoT), vehicular networking systems, and unmanned aerial navigation systems. It is showing promise as a new beamforming methodology that will extend frequency realization, reduce power consumption, and reduce cost and weight. Ansys HFSS (High Frequency Structure Simulator) is used to simulate behavior of these structures with absorbing boundary conditions (radiating boundary) for a few element array structures [35]. Parametric analysis is performed to determine the proper shape and orientation of these structures to obtain multiple simultaneous low overlapping directional beams.

The remainder of the paper is organized such that in Section 2 quasi-optical beamforming is discussed along with the demonstrations and explanation of performance for vertically oriented dielectric wedges. Section 3 explores beamsteering angle control by varying the tilt angle of the vertical wedges. Section 4 discusses the scalability of these structures to larger antenna arrays. Section 5 explores effects of quasi-optical structures on bandwidth. Section 6 discusses the beamforming for  $H$  principal plane. Section 7 discusses the performance trade-offs of each beamforming technique. The last section provides concluding remarks and possible future directions.

## 2. BEAMFORMING USING VERTICALLY ORIENTED DIELECTRIC WEDGES

Configurations of vertically oriented dielectric wedges have been designed, investigated, and demonstrated to form multiple low overlapping beams. This design improves the gain and impedance matching of the antennas. To demonstrate the effect, the structure is designed for 3-element antennas; the design includes dielectric wedges placed vertically in the near field of the antenna. The arrangement and angle of vertical wedges is carefully chosen for the middle, left, and right antenna in order to achieve three distinct beams. The structure was simulated using absorbing boundary conditions. Antennas are designed on Rogers 5880 substrate with dielectric constant of 2.2 and loss tangent of 0.0009. And the superstrate/dielectric wedges are designed using Rogers 6010 with dielectric constant of 10.2 and loss tangent of 0.0009. Figure 1(a) shows triangular dielectric wedges and microstrip patch antenna elements placed at some angles in the close vicinity of antennas. Figure 1(b) shows the top view of the entire

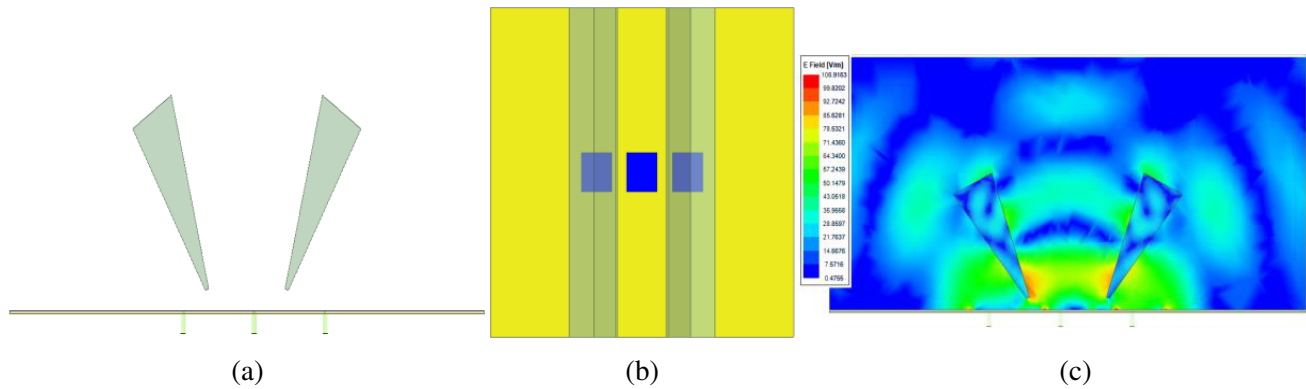


**Figure 1.** (a) Triangular dielectric wedges dielectric placed at some angles in the close vicinity of antennas. (b) Top view of  $1 \times 3$  antenna along with dielectric wedges. (c)  $E$  field plot ( $E$  field lying in the plane shown) for vertical dielectric wedges with all elements excited.

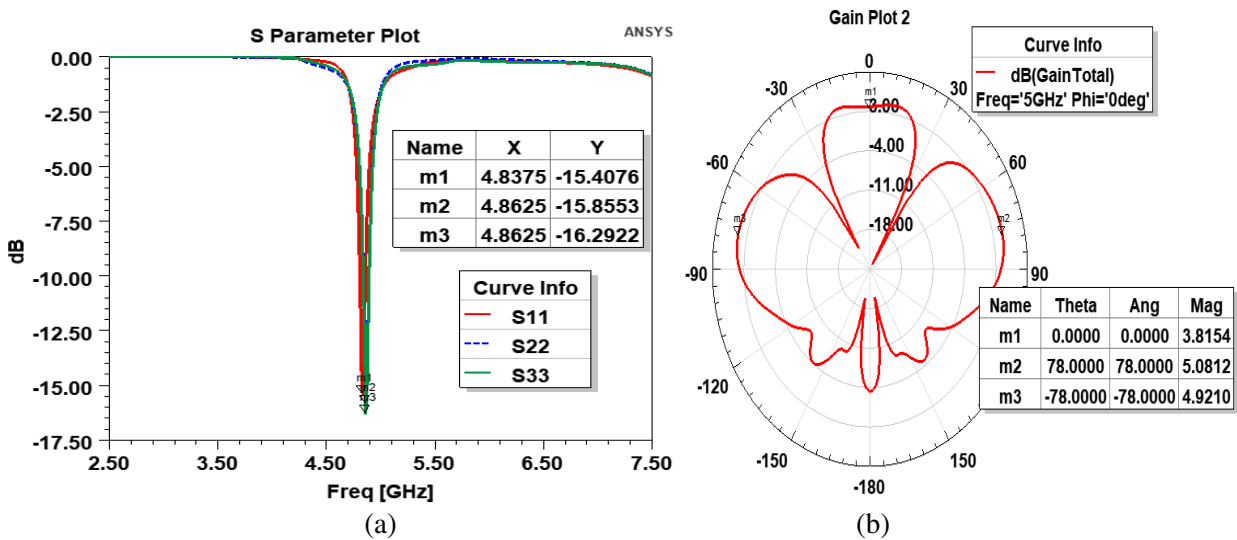


**Figure 2.** (a)  $S$  parameter plot for vertical dielectric wedges. (b)  $E$  principal plane gain plot for vertical dielectric wedges with all elements excited.

design for a  $1 \times 3$  element antenna array along with the dielectric wedges. Figure 1(c) shows the electric field plot when all the antenna elements are active. It can be seen that three distinct low overlapping beams are formed.

Figure 2(a) shows the  $S$  parameter plot where  $S_{11}$  is for the middle antenna,  $S_{22}$  for the left antenna, and  $S_{33}$  for the right antenna. As seen from this figure the impedance matching is good for all antenna elements. Figure 2(b) shows the  $E$  principal plane gain plot for vertical dielectric wedges with all elements excited.

Figures 3(a), (b), (c) show the gain plots for  $E$  principal plane with middle element excited, right element excited, and left element excited, respectively. Notice that Figures 3(a), (b), and (c) show the gain plots from HFSS and CST. The blue curve shows the plot from HFSS, and the red curve shows the plot from CST. It can be clearly seen that the two simulation results are in good agreement. As seen from Figure 3(a) the gain around 11.0 dB with zero beamsteering is achieved when only the middle element is excited. The beam is directive, but it creates two side lobes at different angles. This is caused due to the diffraction from the edges of the vertical dielectric wedges.

Figure 3(b) shows the gain plot of the right element and a gain around 7.8 dB with 80 degrees

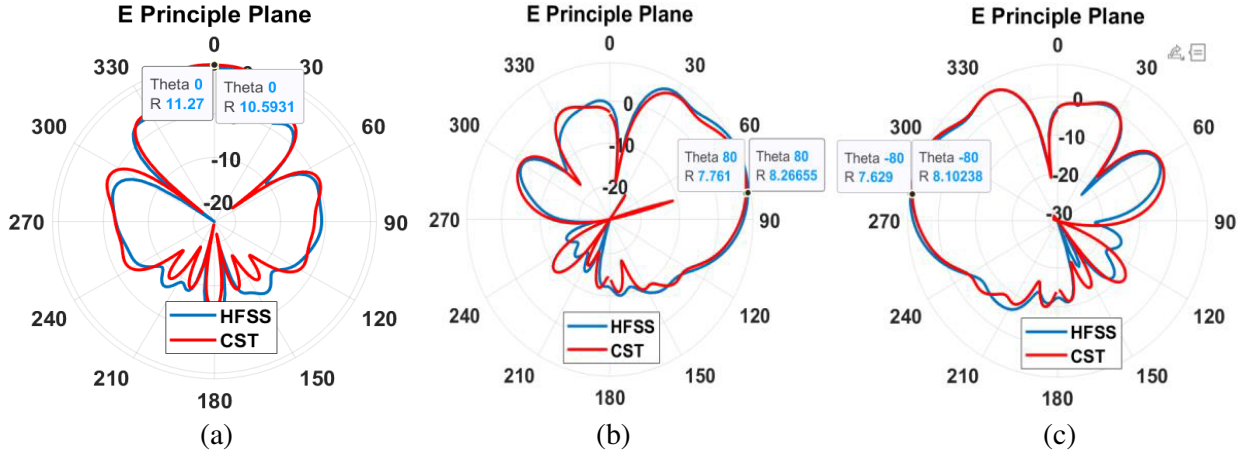


**Figure 3.** (a)  $E$  principal plane gain plot for vertical dielectric wedges with middle element excited. (b)  $E$  principal plane gain plot for vertical dielectric wedges with right element excited. (c)  $E$  principal plane gain plot for vertical dielectric wedges with left element excited.

beamsteering achieved when only the right element is excited. Figure 3(c) shows the gain plot of the left element and a gain around 8.0 dB with  $-80$  degrees beamsteering achieved when only the left element is excited. The steering angle can be varied by changing the dielectric wedge tilting angles as explained in Section 3.

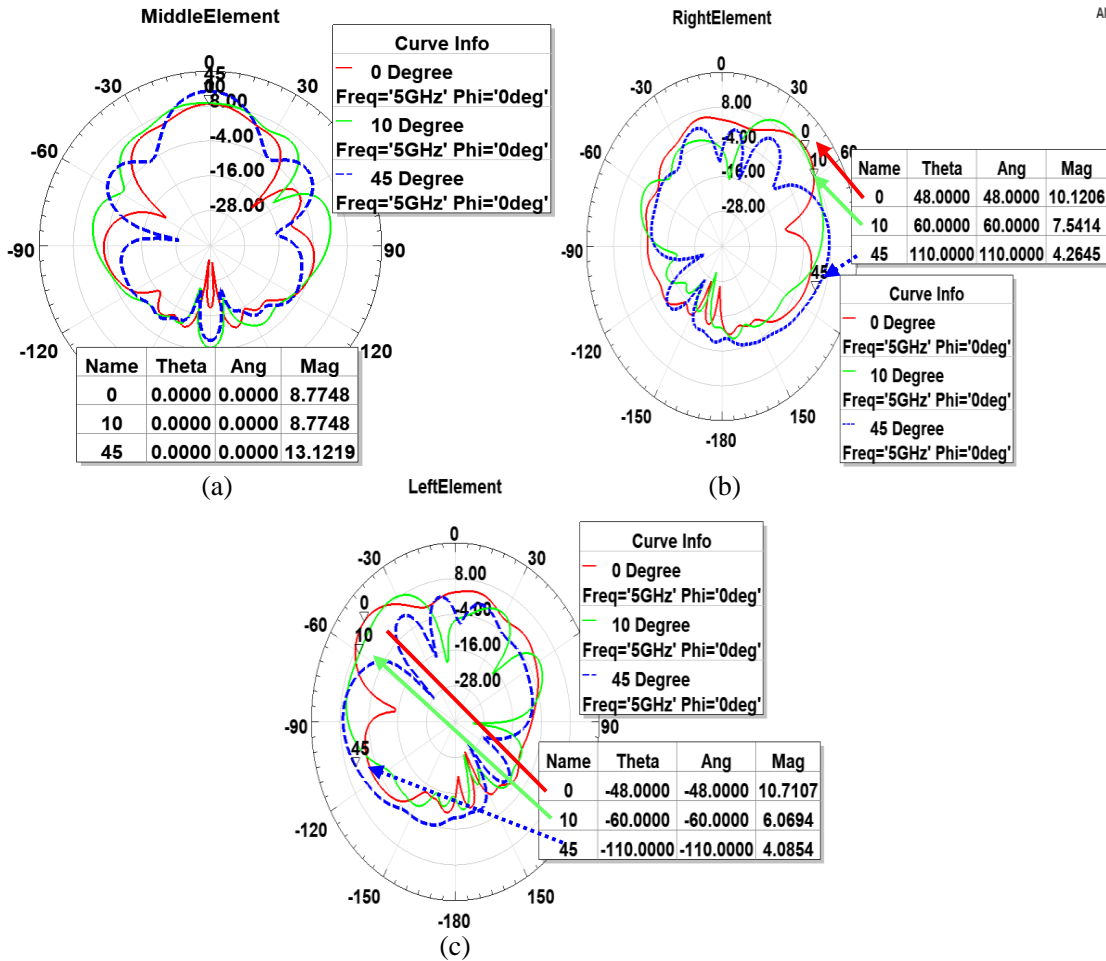
### 3. BEAMSTEERING ANGLE CONTROL

Beamsteering is one of the most important performance features of the proposed beamforming topology. Beamsteering angles can be controlled by varying the tilt angles of the vertically oriented dielectric wedges. The plots for tilt angles of 0 degrees, 10 degrees, and 45 degree are shown. A scanning angle of approximately  $180^\circ$  can be achieved. Note that the dielectric constant of the wedge is kept constant, and only the tilt angle is varied. Figure 4(a) shows the  $E$  principal plane gain plots for vertical dielectric wedge with different tilt angles when the middle antenna element is excited. The figure shows that the gain increases, and the side lobes decrease as the tilt angles increase. The reason behind such behavior can be explained using flaring of the horn antenna as an example. Similarly here, as the flaring (tilt angles) of the wedges increases, a major part of the aperture becomes available to the middle antenna.

Figures 4(b) and 4(c) show the right and left beamsteering gain plots for tilt angles of 0 degrees, 10 degrees, and 45 degrees when right and left elements are excited, respectively. The results in Section 2 are for 20 degrees wedge tilt angles. The dielectric constant of the wedge is kept constant, and only the tilt angle is varied. As seen from these figures, as the tilt angles increases, the beamsteering angle increases, but the gain decreases. The arrows in Figures 4(b) and 4(c) show the maximum gain points on the curves for different angles. Once again referring to the horn antenna angle example, as the flaring (tilt angles) of the wedges increases, the aperture availability for the left and right antenna elements decreases which in turn reduces the gain.

### 4. SCALABILITY

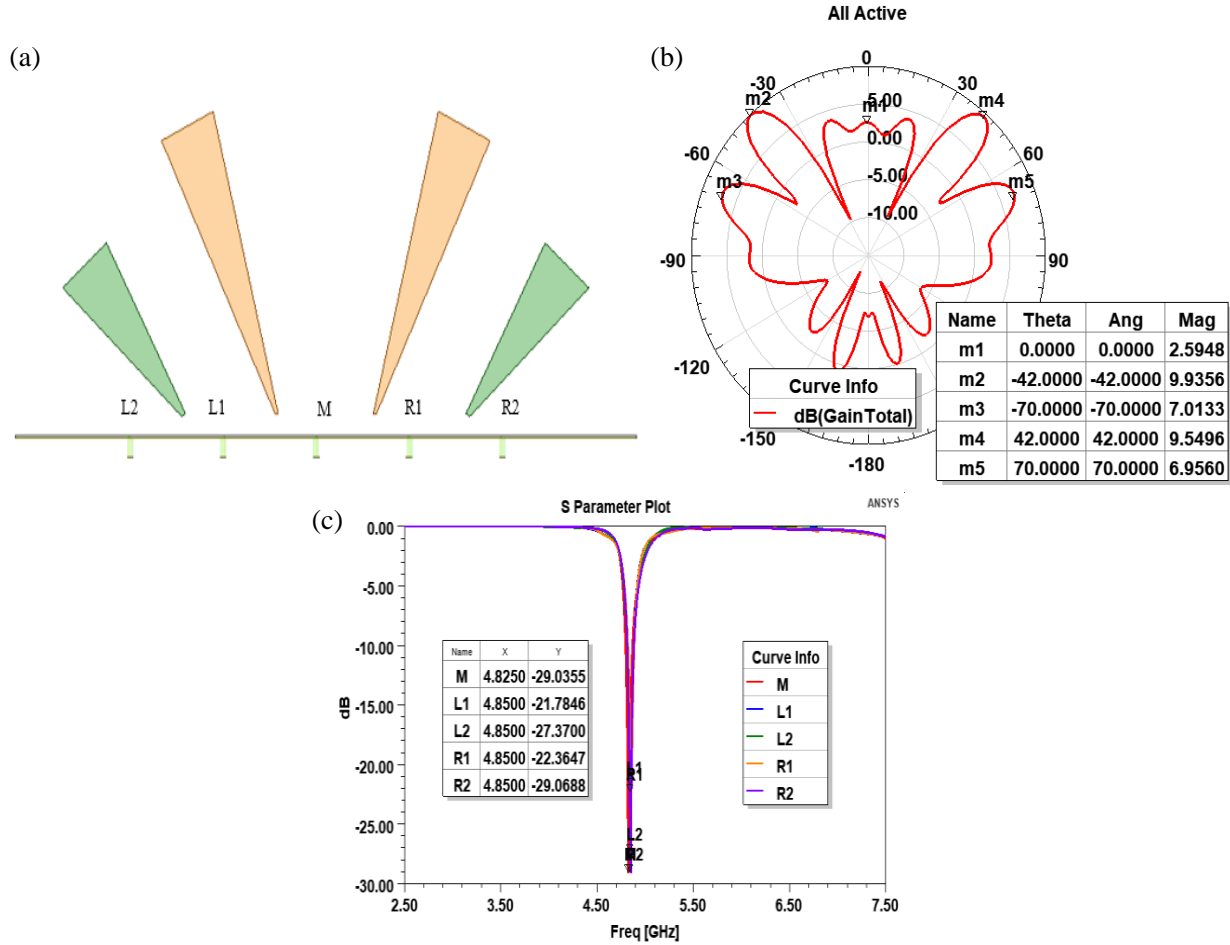
In many communication devices adaptive beamforming antennas are used in order to improve the system performance, reliability, and adaptiveness. Unlike fixed antenna systems, adaptive antennas can adjust their beam shapes and radiation patterns. Ability to satisfy application needs in terms of these parameters in part depends on how effectively the beamformer can scale to larger 1- and 2-dimensional arrays. In this section the ability to scale to larger than  $1 \times 3$  linear arrays, as well as to 2-dimensional arrays is evaluated for the case of vertically oriented dielectric wedges. The ability to scale to larger linear arrays is evaluated by analyzing performance with additional antenna elements and wedges. The



**Figure 4.** (a)  $E$  principal plane gain plots for vertical dielectric wedge with different tilt angles when middle antenna is excited. (b)  $E$  principal plane gain plots for vertical dielectric wedge with different tilt angles when right antenna is excited. (c)  $E$  principal plane gain plots for vertical dielectric wedge with different tilt angles when left antenna is excited.

ability to extend to the 2-dimensional case is considered by ensuring proper beamforming operation in  $H$ -principal plane, in addition to  $E$ -principal plane which has been the focus of earlier sections.

Figure 5(a) shows the arrangement of dielectric wedges for a  $1 \times 5$  microstrip patch antenna. The structure behavior was simulated using absorbing boundary conditions. Two different size wedges are placed on top of the antenna elements. All wedges are designed using Rogers duroid 6010 with dielectric constant of 10.2 and loss tangent of 0.0009. The size of the wedges is carefully designed to obtain five distinct but low overlapping beams. The tilt angle of the orange wedges is 15 degrees, and the tilt angle of the green wedges is 30 degrees. This is designed in such a way that the L1 (first left) antenna and R1 (first right) antennas have sufficient spatial opening to radiate the beam in the required direction. The middle wedges which are denoted with orange color are made large since the beams from antennas L1 and R1 will face multiple reflections between orange and green wedges. The differently sized wedges will give an added advantage to properly steer the beam at the required angle and to obtain distinct beams from antenna elements L1 and R1. The wedge sizes of the extreme wedges are kept smaller since the beams from antennas L2 and R2 will not face any reflections from other wedges. Beams from each antenna can be steered according to the tilt angles of the wedges. Figure 5(b) shows the  $E$  principal plane gain plot for vertical dielectric wedges placed on a  $1 \times 5$  antenna array with all elements excited. Five low overlapping beams are formed. Figure 5(c) shows the  $S$  parameter plots for all of the antennas in the array. As seen from the figure, the impedance matching of all the antennas is good.



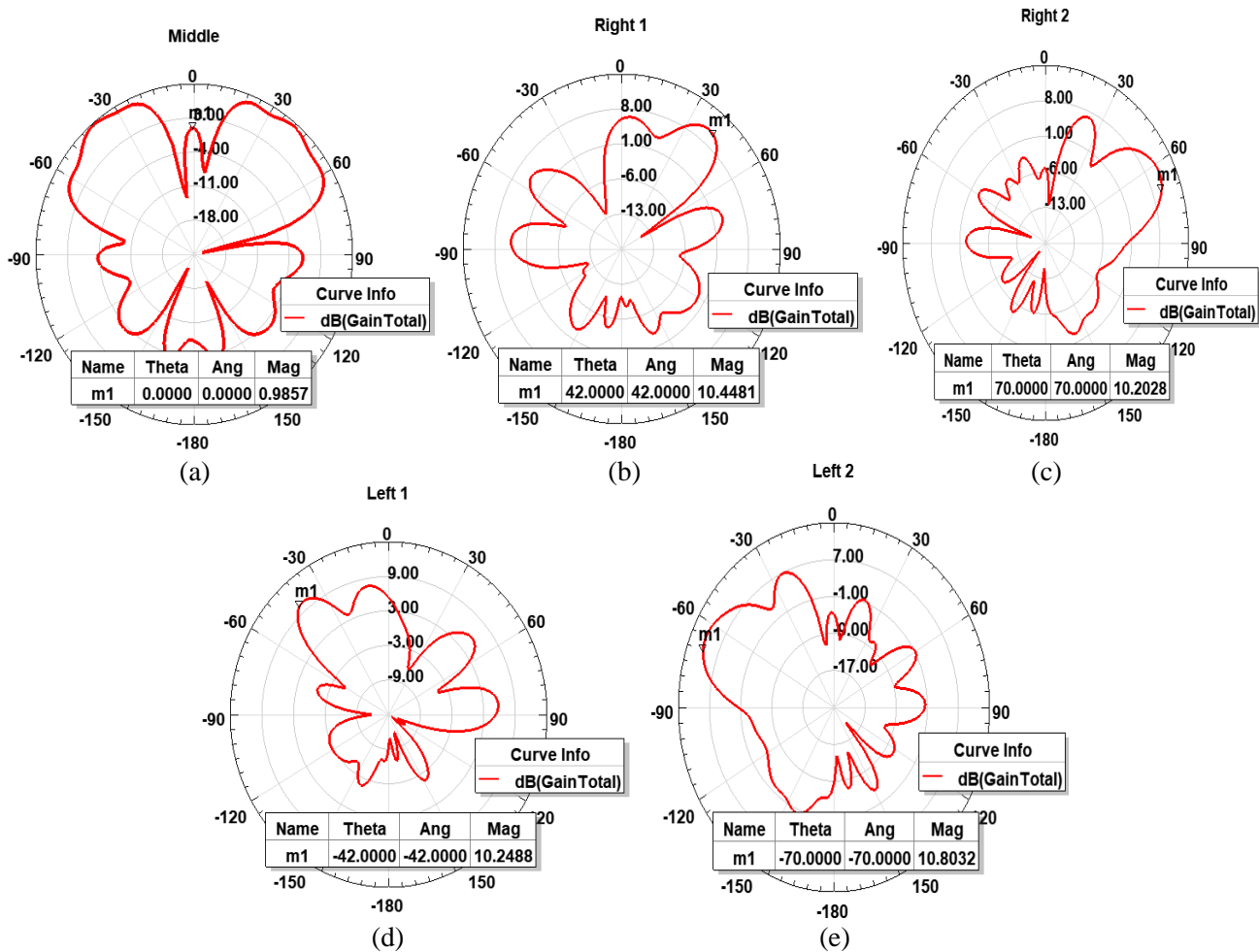
**Figure 5.** (a) Vertical dielectric wedges placed on  $1 \times 5$  antenna. (b)  $E$  principal plane gain plot for vertical dielectric wedges placed on  $1 \times 5$  antenna with all elements excited. (c)  $S$  parameter plot for vertical dielectric wedges placed on  $1 \times 5$  antenna array.

Figure 6 shows gain plots for  $E$  principal plane with each element being excited individually. As seen from Figure 6(a) the gain plot with zero beamsteering is achieved when only the middle element is excited. The beam is directive, but it creates two grating and side lobes at different angles. This is caused by the diffraction occurring at the edges of the middle two wedges (orange color). This is believed to be happening because both the slots of patch antenna element (middle element) are in the near vicinity of the triangular wedge edges. This creates multiple diffraction and refraction effects in the radiating beam. Studies with impedance matching layers are being conducted to address this issue.

Figure 6(b) shows the gain plot for the first right element and a gain of 10.4 dB with 42 degrees beamsteering achieved when only this element is excited. Figure 6(c) shows the gain plot of the second right element and a gain of 10.2 dB with 70 degrees beamsteering achieved when only this element is excited. Figure 6(d) shows the gain plot of the first left element and a gain of 10.2 dB with  $-42$  degrees beamsteering achieved when only this element is excited. Figure 6(e) shows the gain plot of the second left element and a gain of 10.8 dB with  $-70$  degrees beamsteering achieved when only this element is excited.

## 5. EFFECTS ON BANDWIDTH

Various methods have been incorporated to increase the bandwidth of the microstrip patch antenna. For example, lower the  $Q$ -factor of the patch, by using a low dielectric substrate, introducing slots in



**Figure 6.**  $E$  principal plane gain plot for vertical dielectric wedges placed on  $1 \times 5$  antenna when (a) middle element is excited, (b) right 1 element is excited, (c) right 2 element is excited, (d) left 1 element is excited, (e) left 2 element is excited.

the patch or by using a thick dielectric substrate. Researchers have also used defected ground planes or partial ground planes to improve the front to back ratio and suppress surface waves resulting in bandwidth enhancement. To evaluate the effects of vertical dielectric wedges on bandwidth, a  $1 \times 3$  antenna is designed on a thick and low dielectric substrate. The substrate has a thickness of 1.6 mm and a dielectric constant of 1.0. In this section a study is carried out to check the effects on bandwidth by introducing the vertically oriented dielectric wedges. As seen from Figure 7(a), the bandwidth in  $S$  parameter plot is 170 MHz which is 3.4%. In this section a study is carried out to check the effects on bandwidth by introducing the vertically oriented dielectric wedges.

Figures 7(a) and 7(b) show the  $S$  parameter plot where  $S_{11}$  is for the middle antenna,  $S_{22}$  for the left antenna, and  $S_{33}$  for the right antenna. From Figure 7(b) it can be seen that the impedance matching has not changed significantly when the dielectric wedges are added. The  $S_{11}$  plot is highlighted to show the marker readings; the bandwidth can be calculated as 220 MHz, which shows a considerable improvement of 4.4% in the bandwidth. The vertical wedge structure does not exhibit behaviors that would appear to limit bandwidth for a modest bandwidth antenna; however, further study would be needed for wider bandwidth antenna elements. Figure 7(c) shows the  $E$  principal plane gain plots for a thick and low dielectric substrate when all the elements are excited. Not much change is seen from the gain plot compared to the gain plot in Figure 2(b).

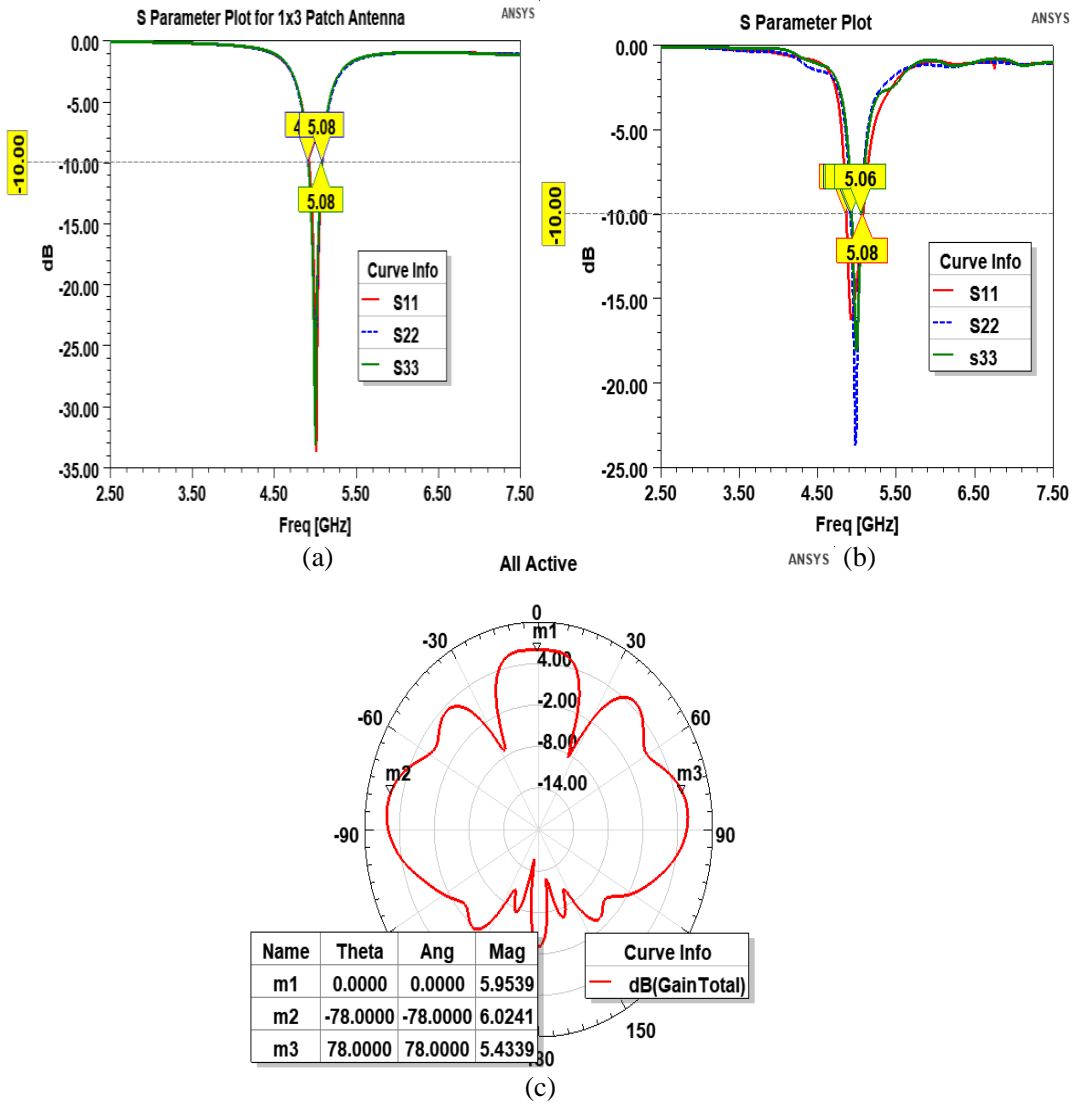


**Figure 7.** (a)  $S$  parameter plot of  $1 \times 3$  patch antenna without dielectric wedges on thick and low dielectric substrate. (b)  $S$  parameter plot of  $1 \times 3$  patch antenna with dielectric wedges on thick and low dielectric substrate. (c)  $E$  principal plane gain plots for thick and low dielectric substrate when all the elements are excited.

### 6. H PRINCIPAL PLANE PLOTS

All the results in the previous sections correspond to the elements arranged in  $E$  principal plane beamforming. In this section the discussion is focused on the structure for  $H$  principal plane beamforming. The design is demonstrated using 3 element antennas, and vertically oriented dielectric wedges. The arrangement and angle of vertical wedges is carefully chosen for the middle, left, and right antenna elements in order to achieve distinct beams. The structure was simulated using absorbing boundary conditions. Antennas were designed using Rogers 5880 substrate with dielectric constant of 2.2 and loss tangent of 0.0009. And superstrate/dielectric wedges are taken to be Rogers 6010 with dielectric constant of 10.2 and loss tangent of 0.0009. Figure 8(a) shows the  $S$  parameter plot where  $S_{11}$  is for the middle antenna,  $S_{22}$  for the left antenna, and  $S_{33}$  for the right antenna. As seen from this figure the impedance matching is good for the entire design.

Figures 8(b), 8(c), and 8(d) show the gain plots for  $H$  principal plane with middle element excited,

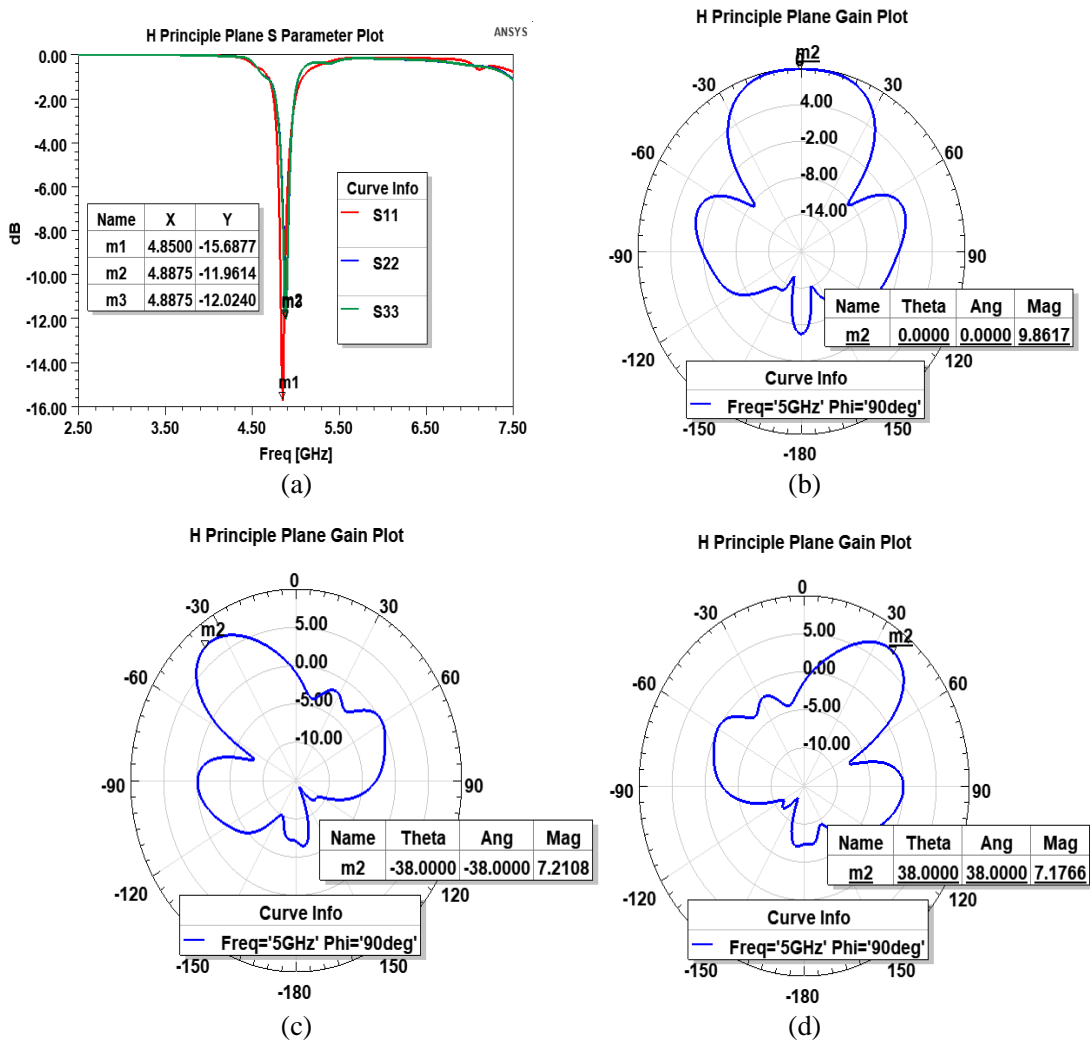


**Figure 8.** (a) *H* principal plane *S* parameter plot for vertical dielectric wedges, (b) *H* principal plane gain plot for vertical dielectric wedges when middle element is excited, (c) when left element is excited, (d) right element is excited.

right element excited, and left element excited, respectively. As seen from Figure 8(b) the gain of 9.9 dB with zero beamsteering is achieved when only the middle element is excited. The beam is directive, but it creates two grating and side lobes at different angles. This is caused by the diffraction effects from the wedges. Figure 8(c) shows the gain plot of left element and a gain of 7.2 dB with  $-38$  degrees beamsteering achieved when only the left element is excited. Figure 8(d) shows the gain plot of right element and a gain of 7.2 dB with 38 degrees beamsteering achieved when only the right element is excited.

### 7. PERFORMANCE TRADE-OFF'S

To summarize the effects of the proposed quasi-optical structure, a comparison table is presented below. Table 1 compares different performance tradeoffs estimations of different beamforming techniques and quasi-optical beamforming structures.

**Table 1.** Performance trade-off table.

Geometries Properties	Digital Beamformer	Analog Beamformer	Microwave Lens Beamformer	Quasi-Optical Beamformer
<b>Gain</b>	Array size dependent	Array size dependent	Array size dependent	Array size dependent
<b>Bandwidth</b>	Narrow band	Wide BW	Wide BW	Wide BW
<b>Operating Frequency</b>	Low mmWave	Low mmWave	High mmWave	High mmWave
<b>Beamsweeping Angle</b>	$\sim 140^\circ$	$\sim 70^\circ$	$\sim 80^\circ$	$\sim 180^\circ$
<b>Scalability</b>	Achievable with more complex digital processing	Achievable up to $8 \times 8$ with low insertion loss	Achievable up to $8 \times 8$ with practically low complexity	Tested up to $7 \times 7$ . Estimated for larger array sizes with high gain
<b>3 dB Beamwidth</b>	Array size dependent	Array size dependent	Array size dependent	Array size dependent
<b>Sidelobe Level</b>	Less than $-10$ dB	Less than $-5$ dB	Less than $-5$ dB	Less than $-2$ dB
<b>Power Supplied</b>	High	None/Low	None/Low	None/Low
<b>Insertion Loss</b>	Low	High	High	Low
<b>Cost and Complexity</b>	Expensive and complex	Expensive and practically limited complexity	Relatively expensive and practically limited complexity	Relatively inexpensive and low complexity

## 8. CONCLUSION

This paper presents a state-of-the-art quasi-optical beamforming approach that will reduce the size, cost, and power consumption considerably. The arrangement of vertically oriented dielectric wedges placed over the array of patches generates distinct multiple simultaneous low overlapping beams. This arrangement improved the gain and bandwidth of the entire design. Beamsteering angle control was demonstrated by varying the tilt angle of dielectric wedges, and the beamsweeping angle of  $180^\circ$  was achieved. The proposed design is scalable, and scalability was demonstrated for  $1 \times 5$  antenna array and for  $H$  principal plane. Using the proposed method this technique can be extended to larger linear and 2D arrays.

## REFERENCES

1. Balanis, C. A., *Antenna Theory: Analysis and Design*, John Wiley & Sons, 2016.
2. Hansen, R. C., *Phased Array Antennas*, Vol. 213, John Wiley & Sons, 2009.
3. Maharimi, S. F., et al., "Impact of number elements on array factor in linear arrays antenna," *2012 IEEE 8th International Colloquium on Signal Processing and Its Applications*, IEEE, Malacca, Malaysia, 2012.
4. Ehyai, D., "Novel approaches to the design of phased array antennas," Dissertation, 2011.
5. Ulaby, F. T., E. Michielssen, and U. Ravaioli, *Fundamentals of Applied Electromagnetics*, 6th Edition, Prentice Hall, Boston, Massachusetts, 2010.

6. Rotman, W. and R. Turner, "Wide-angle microwave lens for line source applications," *IEEE Transactions on Antennas and Propagation*, Vol. 11, No. 6, 623–632, 1963.
7. Zaghloul, A. I. and E. D. Adler, "Compact Rotman lens using metamaterials," U.S. Patent No. 8,736,503, May 27, 2014.
8. Dong, J. and A. I. Zaghloul, "Hybrid ray tracing method for microwave lens simulation," *IEEE Transactions on Antennas and Propagation*, Vol. 59, No. 10, 3786–3796, 2011.
9. Hansen, R. C., "Design trades for Rotman lenses," *IEEE Transactions on Antennas and Propagation*, Vol. 39, No. 4, 464–472, 1991.
10. Moody, H., "The systematic design of the Butler matrix," *IEEE Transactions on Antennas and Propagation*, Vol. 12, No. 6, 786–788, 1964.
11. Belkin, M. E., et al., "Design of reconfigurable multiple-beam array feed network based on millimeter-wave photonics beamformers," *Advances in Array Optimization*, InTechOpen, 2019.
12. Butler, J. L., "Multiple beam antenna system employing multiple directional couplers in the leadin," U.S. Patent No. 3,255,450, Jun. 7, 1966.
13. Uchendu, I. and J. R. Kelly, "Survey of beam steering techniques available for millimeter wave applications," *Progress In Electromagnetics Research B*, Vol. 68, 35–54, 2016.
14. Ruze, J., "Wide-angle metal-plate optics," *Proceedings of the IRE*, Vol. 38, No. 1, 53–59, 1950.
15. Kalam, S. V. and A. B. Rathi, "Optimum design of  $4 \times 4$  symmetrically structured Butler matrix," *International Journal of Scientific Research Engineering*, 31–34, 2016.
16. Barry, J., et al., " $4 \times 4$  X-band butler matrices as antenna beamformers," *Multi-Disciplinary Senior Design Conference*, Project No. P09343, 2009.
17. Kim, J.-H., et al., "Design of phased array antenna for 5G mm-wave beamforming system," *2016 IEEE 5th Asia-Pacific Conference on Antennas and Propagation (APCAP)*, IEEE, 2016.
18. Charczenko, W., et al., "Integrated optical Butler matrix for beam forming in phased-array antennas," *Optoelectronic Signal Processing for Phased-Array Antennas II*, Vol. 1217, International Society for Optics and Photonics, 1990.
19. Hock, G. C., et al., "Rapid and simple design approach of micro-strip Butler matrix beam-forming network for wireless system," *IEICE Electronics Express*, Vol. 9, No. 5, 346–351, 2012.
20. Ibrahim, A. Z. and M. K. A. Rahim, "Comparison between three radiation pattern using Butler matrix for beamforming network," *Jurnal Teknologi*, Vol. 54, No. 1, 25–43, 2011.
21. Mosca, S., et al., "A novel design method for Blass matrix beam-forming networks," *IEEE Transactions on Antennas and Propagation*, Vol. 50, No. 2, 225–232, 2002.
22. Casini, F., et al., "A novel design method for Blass matrix beam-forming networks," *2007 European Microwave Conference*, IEEE, 2007.
23. Attia, H., "Artificial magnetic materials for high gain planar antennas," Theses, University of Waterloo, 2011.
24. Konstantinidis, K., "Multi-layer periodic surfaces and metasurfaces for high-gain antennas," Dissertation, University of Birmingham, 2015.
25. Debogović, T., "Dynamic beamwidth control in partially reflective surface antennas," *Proceedings of the 33rd ESA Antenna Workshop on Challenges for Space Antenna Systems*, 2011.
26. Jackson, D. and N. Alexopoulos, "Gain enhancement methods for printed circuit antennas," *IEEE Transactions on Antennas and Propagation*, Vol. 33, No. 9, 976–987, 1985.
27. James, J. R., et al., "Leaky-wave multiple dichroic beamformers," *Electronics Letters*, Vol. 25, No. 18, 1209–1211, 1989.
28. Feresidis, A. P. and J. C. Vardaxoglou, "High gain planar antenna using optimised partially reflective surfaces," *IEE Proceedings — Microwaves, Antennas and Propagation*, Vol. 148, No. 6, 345–350, 2001.
29. Feresidis, A. and J. C. Vardaxoglou, "Flat plate millimetre wave antenna based on partially reflective FSS," *2001 Eleventh International Conference on Antennas and Propagation, (IEE Conf. Publ. No. 480)*, Vol. 1, IET, 2001.

30. Arora, C., S. S. Pattnaik, and R. N. Baral, "SRR superstrate for gain and bandwidth enhancement of microstrip patch antenna array," *Progress In Electromagnetics Research B*, Vol. 76, 73–85, 2017.
31. Khan, M. R., "A beam steering technique using dielectric wedges," Dissertation, University of London, 1995.
32. Von Trentini, G., "Partially reflecting sheet arrays," *IRE Transactions on Antennas and Propagation*, Vol. 4, No. 4, 666–671, 1956.
33. Ghate, P. and J. Bredow, "Beam deflection using non-planar broadside coupled split ring resonators," *2020 IEEE Asia-Pacific Microwave Conference (APMC)*, 245–247, Hong Kong, 2020, doi: 10.1109/APMC47863.2020.9331402.
34. Afzal, M. U., et al., "Beam-scanning antenna based on near-electric field phase transformation and refraction of electromagnetic wave through dielectric structures," *IEEE Access*, Vol. 8, 199242–199253, 2020.
35. <https://www.ansys.com/products/electronics/ansys-hfss>.